Defence Research and Development Canada
Recherche et développement pour la défense Canada

A Uniform, Reproducible and Tunable SERS Substrate for Chemical and Biological Sensing

Shiliang Wang
DRDC Suffield

Lilin Tay
National Research Council Canada

Henry Liu
DRDC Suffield

Defence R&D Canada

Technical Memorandum
DRDC Suffield TM 2012-164

November 2013

A Uniform, Reproducible and Tunable SERS Substrate for Chemical and Biological Sensing

Shiliang Wang
DRDC Suffield

Lilin Tay
National Research Council Canada

Henry Liu
DRDC Suffield

Defence R&D Canada – Suffield

Technical Memorandum
DRDC Suffield TM 2012-164
November 2013

Principal Author

Original signed by Shiliang Wang

Shiliang Wang

Defence Scientist

Approved by

Original signed by Scott Duncan

Scott Duncan

H/HPS

Approved for release by

Original signed by Robin Clewley

Robin Clewley

Chair/DRP

Abstract

This report provides a novel approach to self-assembled negatively charged individual pristine silver nanoparticles generated in the gas phase (with diameter less than 10 nm) on to a solid support (glass, plastic, rubber, silicon wafer, indium tin oxide, etc.) for the fabrication of a low-cost surface enhanced Raman spectroscopy (SERS) substrate. The SERS substrate has been demonstrated to be tunable to accommodate different excitation lasers to achieve the maximum SERS response simply by controlling the deposition time. The SERS response has been shown to be highly reproducible and uniform from point-to-point across the entire substrate as well as from batch-to-batch, which is desirable for quantifiable detection of chemical and biological molecules. In addition, the DRDC SERS substrate works well for chemical and biochemical sensing in both liquid and vapour forms. This new technology may provide an affordable and reliable sensing and identification capability against new and emerging chemical and biological threats such as non-traditional agents (NTAs) in support of the Canadian Forces (CF).

Résumé

Le présent rapport fournit une nouvelle approche concernant les nanoparticules d'argent pures individuelles chargées négativement et auto assemblées produites au cours de la phase gazeuse (diamètre de moins de 10 nm) sur un support solide (verre, plastique, caoutchouc, plaquette de silicium, oxyde d'étain et d'indium, etc.) pour la fabrication d'un substrat SERS (spectrométrie Raman améliorée par la surface) peu coûteux. On a démontré que le substrat SERS est réglable afin de pouvoir s'adapter à différents lasers d'excitation pour obtenir la réponse SERS maximale simplement en contrôlant le temps de dépôt. On a démontré que la réponse SERS est hautement reproductible et uniforme d'un point à l'autre dans tout le substrat et d'un échantillon à l'autre, ce qui est souhaitable pour la détection quantifiable de molécules chimiques et de molécules biologiques. De plus, le substrat SERS de RDDC est efficace pour la détection chimique et la détection biochimique sous forme liquide et sous forme de vapeur. Cette nouvelle technologie peut fournir une capacité d'identification et de détection fiable et abordable des menaces biologiques et des menaces chimiques nouvelles ou émergentes comme les agents non traditionnels (ANT) pour appuyer les Forces canadiennes (FC).

This page intentionally left blank.

Executive Summary

A Uniform, Reproducible and Tunable SERS Substrate for Chemical and Biological Sensing

Shiliang Wang; Lilin Tay; Henry Liu; DRDC Suffield TM 2012-164; Defence R&D Canada – Suffield; November 2013.

Introduction or background: A future goal of DRDC Suffield's chemical defence S&T programme is to develop a sensor that is capable of rapidly detecting and identifying new and emerging chemical/biological threats such as non-traditional agents (NTAs) under ambient exposure conditions and very low mass concentrations to allow the CF to make informed decisions on the agent present and the type of response and mitigation measures that they will have to put in place to maintain their operational tempo. Raman spectroscopy measures the shift in energy from interrogating laser light to determine information about the vibrational fingerprints of hazard materials. Since its discovery in the 70s, surface enhanced Raman spectroscopy (SERS) has reached a sensitivity down to the level of single molecule detection and has tremendously benefited from advances in nanoscience and nanotechnology. A primary factor that has hindered commercial adoption of this technology is the lack of affordable, uniform and reproducible SERS-active substrates. DRDC Suffield has developed a simple approach for low cost, uniform, reproducible and tunable SERS substrates for chemical and biochemical sensing.

Results: We have developed a technique to self-assemble negatively charged individual pristine silver nanoparticles generated in the gas phase (with diameter less than 10 nm) on to a solid support (glass, plastic, rubber, silicon wafer, indium tin oxide, etc.) for the preparation of SERS-active substrates. The deposition process yields ensembles with average interparticle spacing that decreases steadily as a function of deposition time. The localized surface plasmon resonance (LSPR), on which SERS enhancement relies, can be tuned to any wavelength in the visible range (385-800 nm) by controlling the deposition time. The correlation between the laser excitation wavelength and the maximum of LSPR shows that this approach can provide SERS substrates tailored to different excitation lasers. The DRDC SERS substrates fabricated with this approach exhibit good reproducibility and uniformity from point-to-point as well as from batch-to-batch, which is desirable for quantifiable detection of chemical and biological molecules. In addition, the DRDC SERS substrate provides a versatile SERS substrate platform for chemical and biochemical sensing in both liquid and vapour forms, one-step closer towards our goal to provide a complete chemical nanosensor.

Significance: The collaboration between DRDC Suffield and NRC-MMS has created a tunable, uniform and reproducible SERS substrate platform for chemical and biochemical detection and identification. We provide an affordable and reliable sensing and identification capability against new and emerging chemical threats in support of the CF. The impacts of this research extend beyond the military to public safety and public health. The new technology offers a tool for investigating trace chemical exposure and accumulation in the environment. This document will support a patent application to USPTO.

Future plans: Efforts toward a portable device for chemical and biochemical hazards sensing are underway in support of CF.

Sommaire

A Uniform, Reproducible and Tunable SERS Substrate for Chemical and Biological Sensing

Shiliang Wang; Lilin Tay; Henry Liu ; DRDC Suffield TM 2012-164 ; R & D pour la défense Canada – Suffield; novembre 2013.

Introduction : L'un des objectifs du programme de science et de technologie concernant la défense chimique de RDDC Suffield est de concevoir un capteur pouvant détecter et identifier rapidement les menaces chimiques/biologiques nouvelles ou émergentes comme les agents non traditionnels (ANT) dans des conditions d'exposition ambiantes et des concentrations en masse très faibles pour permettre aux FC de prendre des décisions éclairées concernant l'agent présent et le type de réponse et de mesures d'amoindrissement qu'elles devront mettre en place pour maintenir leur vitesse opérationnelle. La spectrométrie Raman mesure la variation d'énergie émise par la lumière laser d'interrogation pour déterminer l'information concernant les empreintes vibrationnelles des matières dangereuses. Depuis sa découverte dans les années 70, la spectrométrie Raman améliorée par la surface (SERS) a atteint une sensibilité lui permettant de détecter chacune des molécules, et a profité énormément des percées en nanoscience et en nanotechnologie. L'un des principaux facteurs qui ont nui à l'adoption commerciale de cette technologie est le manque de substrats SERS actifs abordables, uniformes et reproductibles. RDDC Suffield a conçu une approche simple concernant les substrats SERS réglables, reproductibles, uniformes et peu coûteux pour la détection chimique et la détection biologique.

Résultats : Nous avons élaboré une technique permettant d'auto assembler les nanoparticules d'argent pures individuelles chargées négativement produites au cours de la phase gazeuse (diamètre de moins de 10 nm) sur un support solide (verre, plastique, caoutchouc, plaquette de silicium, oxyde d'étain et d'indium, etc.) pour la préparation de substrats SERS actifs. Le processus de dépôt produit des ensembles ayant un espace moyen entre les particules qui diminue de façon régulière en fonction du temps de dépôt. La résonance plasmonique de surface localisée (RPSL), à laquelle l'amélioration grâce à la SERS se fie, peut être réglée à n'importe quelle longueur d'onde dans la plage du visible (de 385 à 800 nm) en contrôlant le temps de dépôt. Le lien entre la longueur d'onde d'excitation par laser et la RPSL maximale montre que cette approche peut fournir des substrats SERS adaptés à différents lasers d'excitation. Les substrats SERS de RDDC fabriqués en utilisant cette approche ont une bonne reproductibilité et une bonne uniformité d'un point à l'autre et d'un échantillon à l'autre, ce qui est souhaitable pour la détection quantifiable de molécules chimiques et de molécules biologiques. De plus, le substrat SERS de RDDC fournit une plate forme polyvalente pour la détection chimique et la détection biologique sous forme liquide et sous forme de vapeur, ce qui nous rapproche un peu plus de notre but, qui est de fournir un nanocapteur chimique complet.

Portée : La collaboration entre RDDC Suffield et NRC-MMS a permis de créer une plate forme réglable, uniforme et reproductible pour la détection et l'identification chimiques ou biochimiques. Nous fournissons une capacité de détection et d'identification abordable et fiable des menaces chimiques nouvelles ou émergentes pour appuyer les FC. Les conséquences de cette recherche dépassent le domaine militaire; elles vont jusqu'à la santé publique et la sécurité publique. La nouvelle technologie offre un outil permettant d'étudier l'exposition à des traces de produits chimiques et l'accumulation de ces produits chimiques dans l'environnement. Ce document appuiera une demande brevet faite à l'USPTO.

Recherches futures : On tente présentement de créer un dispositif portatif de détection de dangers chimiques ou biochimiques pour appuyer les FC.

Table of Contents

List of Figures

List of Tables

Introduction

Since its discovery in the 70s [1][2][3][4], surface enhanced Raman spectroscopy (SERS) has reached a sensitivity down to the level of single molecule detection. A primary factor that has hindered commercial adoption of this technology is the lack of affordable, uniform and reproducible SERS-active substrates. SERS has benefited tremendously from the advances in nanoscience and nanotechnology in recent decades [5][6][7]. With properly-designed plasmonic nanostructures, SERS is capable of detecting very few molecules and identifying them based on their vibrational fingerprint. Raman signal amplification in SERS is largely due to the enhancement of the electromagnetic fields in the close proximity of the metal nanostructures [8][9][10]. Other contributions such as chemical enhancement [11] due to metal-to-molecule charge transfer effects that result from the formation of molecule-metal interactions also affect the Raman scattering cross-sections. When light of appropriate frequency is incident on metallic nanostructures, the collective excitation of the conduction electron in the metallic nanostructure results in the form of dipolar localized surface plasmon. This causes the incident and scattered electromagnetic fields to be concentrated to a very small region of the nanostructure. Molecule polarizability is greatly amplified in this region of the highly localized field. This amplification can be further strengthened by coupling to nanostructures so as to allow them to interact with the localized surface plasmon resonance. Such coupling is the key to attaining extremely large SERS enhancement factors that are critical for ultrasensitive detection of analytes. Thus, the most SERS-active substrates typically consist of tightly-coupled metal nanoparticle systems. Under optimal conditions, the coupling of LSPR in nanoparticle assemblies is capable of sustaining an extremely intense electric field strength (with SERS enhancement factors exceeding 10^9) thus enabling detection of a single molecule [12][13].

Uniformity and reproducibility of the SERS-active substrate are essential for quantitative detection. Lithographically produced SERS substrates are commercially available. This process allows fine morphological control over the size and shape of the nanostructured surface. The disadvantage is that the fabrication process is very time consuming and the cost of production is high. In addition, there is a lower limit to the size of the nanostructure that can be fabricated via a lithographic technique.

In this article, we report a bottom-up approach for the preparation of SERS-active substrates. We have recently developed a technique to self-assemble negatively charged individual pristine silver nanoparticles generated in the gas phase (with diameter less than 10 nm) on to a solid support (glass, plastic, rubber, silicon wafer, indium tin oxide, etc.). The deposition process yields ensembles with average interparticle spacing that decreases steadily as a function of deposition time. The LSPR can be tuned to any wavelength in the visible range (385-800 nm) by controlling the deposition time. In comparison with vapour deposited metal islands, the maximum enhancement of the SERS-active substrates prepared with our approach correlated with LSPR peak position. In addition, pristine SERS-active substrates fabricated with this approach exhibit good surface uniformity and reproducible SERS enhancement factors, which are consistent from batch to batch.

This page intentionally left blank.

Experimental

Negatively charged silver nanoparticles were prepared in the gas phase using a DC magnetron sputtering source (Nanogen50, Mantis) described elsewhere [14]. Briefly, a 50.8 mm diameter Ag target (Alfa Aesar, 99.99%) was attached to the sputter head, which acted as the cathode, and a voltage was applied between it and the anode cap situated 5 mm away. Ar gas was introduced at a flow rate of 50 sccm (MKS 1179 gas flow controller) through a showerhead inlet directed at the anode cap and positioned immediately in front of the anode cap. The Ag metal atoms sputtered by the discharge left the plasma region through a 46 mm diameter hole in the center of the anode cap. The metal vapour then entered the aggregation zone where condensation and formation of negatively charged Ag nanoparticle occurred. Through a separate gas inlet, a 10 sccm flow of helium was introduced into the aggregation zone to facilitate the condensation and nanoparticle formation. The nanoparticles then entered a secondary aggregation zone evacuated by a 500 Ls^{-1} turbo pump (Varian V-550) and subsequently passed through an orifice into the deposition chamber where a pressure of $<10^{-4}$ torr was maintained during deposition by a 300 Ls^{-1} turbo pump (Varian TV-301). The negatively charged nanoparticles were collected on plain glass substrates, p-dopped silicon wafer or glass slides. These substrates were pre-patterned with two parallel strips of Ag electrodes separated by a 3 mm gap. The substrates were placed 2 cm from the orifice directly in the nanoparticle beam path. The size distribution of the gas phase generated nanoparticles was measured with a quadruple mass filter (MesoQ, Mantis).

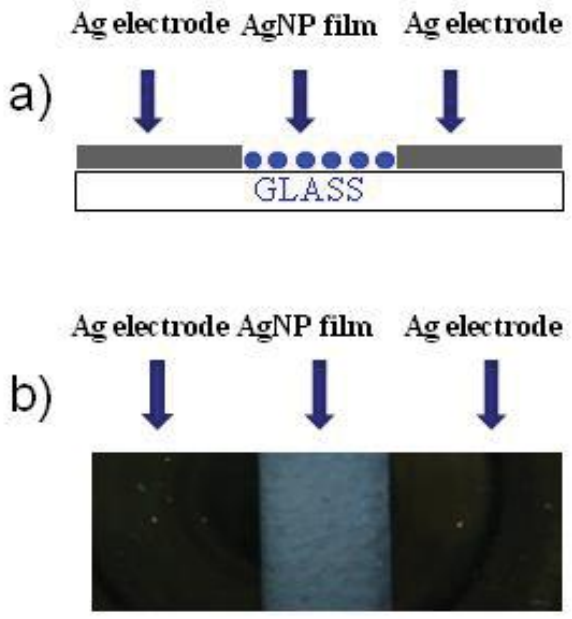

Figure 1 a) a schematic and b) a picture of SRES substrate.

Atomic force microscopy (AFM) was performed with a Veeco MultiMode™ AFM operated in tapping mode. The AFM images were acquired at a horizontal scan rate of 0.5 μms^{-1} using a Si tip

on a cantilever with a nominal spring constant of 42 Nm^{-1} and a nominal resonant frequency of 320 kHz.

Scanning Electron Microscopy (SEM) was performed with a Hitachi S-4700 field-emission scanning electron microscope. All substrates were imaged with an acceleration voltage of 5 keV at a working distance of 4.8 mm. As Ag nanostructures have a tendency to degrade under electron beam irradiation all imaging conditions were first optimized with features outside of the imaged area. The beam was then rastered over the region of interest once only to generate the final image.

Raman spectra were acquired with microRaman spectrometers (LabRAM HR from Horiba Jobin Yvon at NRC and Xplorer from Horiba Jobin Yvon at DRDC). At NRC, SERS spectra were taken with 532 nm and 633 nm radiation, coupled through a 100X objective. At DRDC, SERS spectra were recorded with 532 nm and 785 nm laser excitation, coupled through a 100X objective. While acquisition time varied from substrate to substrate, all spectra detailed in the reports are listed in the unit of counts per second (cps) to account for this variation.

Results and Discussion

2-D Pristine Silver Nanoparticles Film Substrate for SERS

The size of the gas phase generated nanoparticles can be controlled by varying the magnetron distance as shown in Fig. 2. The Ag nanoparticles are monodispersed, as seen in the inset. The size of the Ag nanoparticle was found to be 3.9 ± 0.6 nm in diameter at magnetron distance of 20 mm. Extrapolating the magnetron distance to 0 mm, the peaking size of the nanoparticle is 3.0 ± 0.4 nm, in agreement with the STM measurement of 3.0 ± 0.5 [14]. All SERS substrates in this report were prepared with magnetron distance at 0 mm.

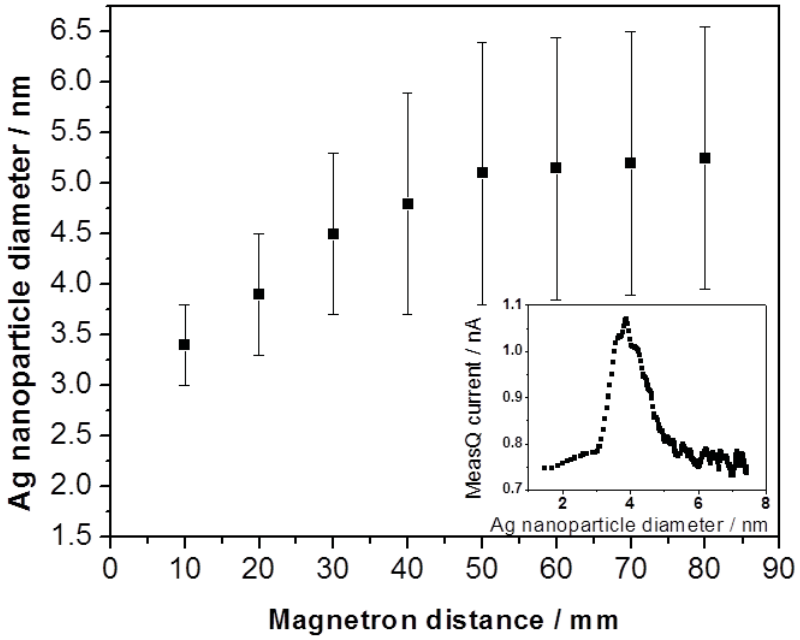

Figure 2 Plot of Ag nanoparticle size as a function of the magnetron distance. The inset displays the size distribution at magnetron distance of 20 mm.

Fig. 3 is the SEM image of a low density SERS substrate deposited with 3.0 ± 0.4 nm silver nanoparticles on a Si support. The nanoparticles are monodispersed, consisting of distinct individual particles, most of which are spheroidal. The size of Ag nanoparticles in the SEM image peaks at 4.5 ± 0.5 nm, as seen in the size distribution graph shown in the inset of Fig. 3. Larger nanoparticle sizes measured with SEM may be attributed to particle coalescence caused by electron beam irradiation during the imaging process [16]. Other mechanisms may also contribute to the coalescence of nanoparticles on the solid support [15]. In contrast to various atomic vapour deposition methods where the irregular metal islands or non-monodispersed nanoparticles are formed on the solid support after atomic species landed on it, monodispersed metal nanoparticles are formed in the gas phase before deposition on a solid support in this approach. The density of nanoparticles on the substrates could easily be controlled by varying the deposition time. Longer deposition times yields more nanoparticles on the substrates, which increases the particle density thus decreases the average distance between neighbouring particles.

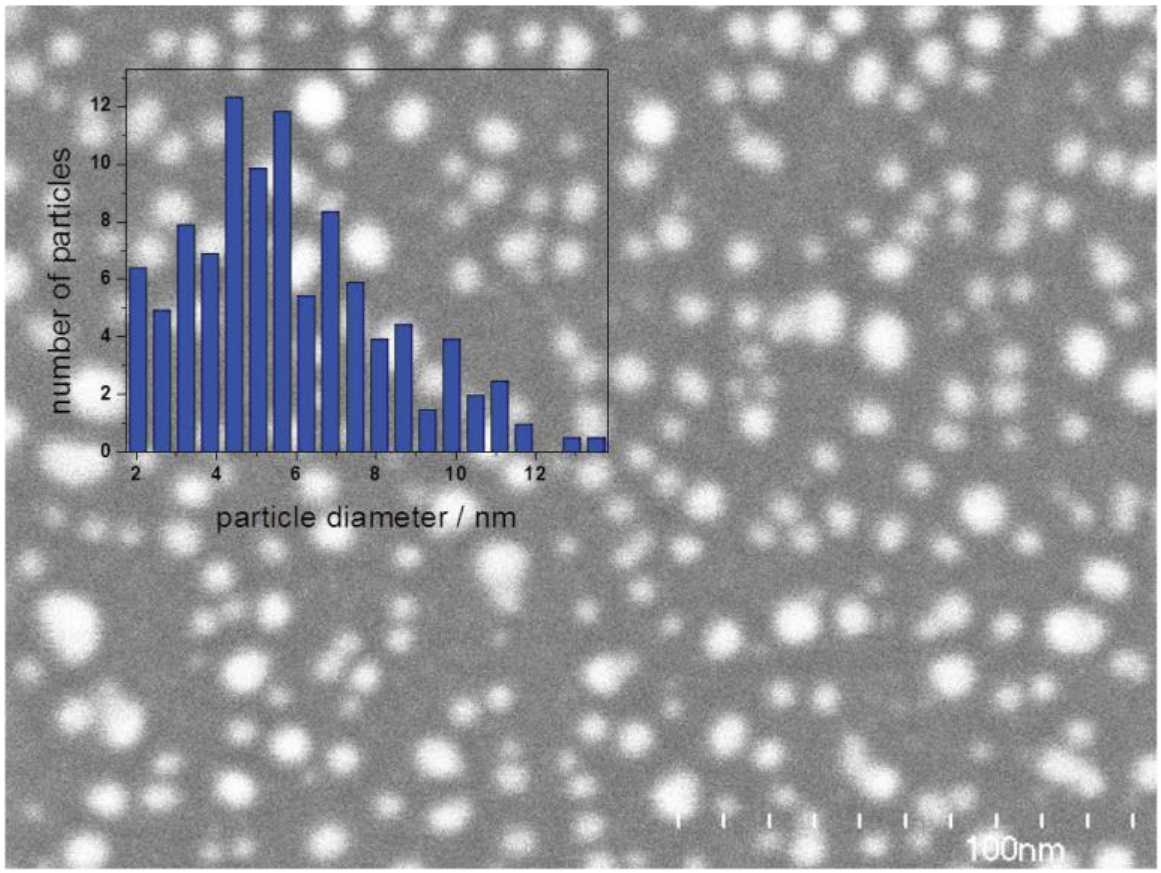

Figure 3 Low density Ag nanoparticle SERS substrate on p-dopped Si wafer support (substrate 1)

Fig 4 showed the AFM and SEM images of a high density SERS substrate (substrate 2) deposited close to percolation threshold on glass slide. As shown in Fig. 4a, the nanoparticles are monodispersed and retain their individuality. As the nanoparticles generated in the gas phase by the plasma source are known to be singly charged negative ions: the Coulomb force between nanoparticles is sufficiently repulsive to prevent aggregation or coalescence during the deposition process. In contrast to colloidal metal nanoparticles, we do not rely on chemical "shell" such as capping agents or insulating material in the self-assembly of the film. This is consistent with our previous observation that SERS substrates prepared through this process consists of close-packed pristine metal nanoparticles.

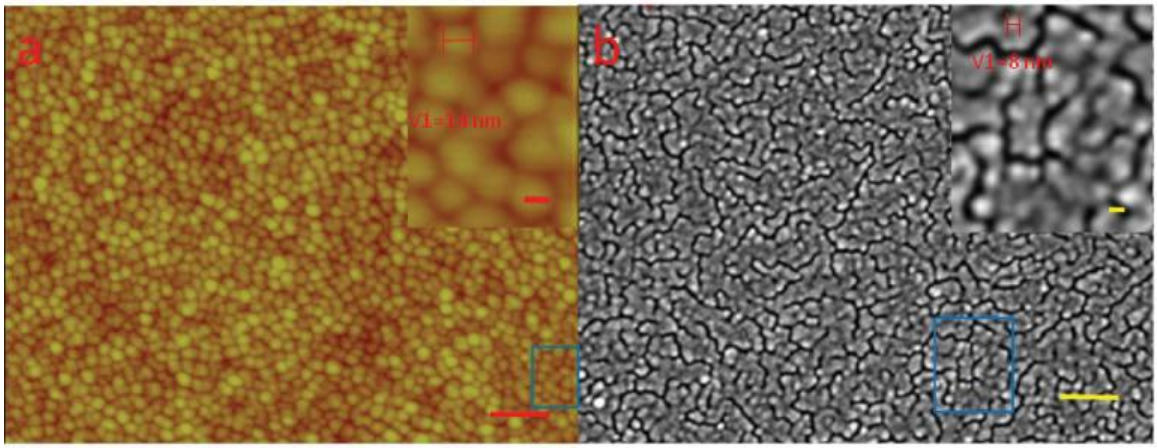

Figure 4 (a) AFM image and (b) SEM image of a high density Ag NPs films on glass slide (substrate 2, 7x7 mm). The scale bars shown in (a) and (b) are 100 nm . To better view the particle topography of the nanoparticle film, sections of each image, outlined with blue boxes, are shown at higher magnification in the insets. Scale bars in both insets are 10 nm.

It is known that the lateral dimension of nanostructures as measured by AFM tends to be larger than the real value due to the limit size of the AFM tips, normally around 10 nm. For smaller nanostructures (less than 10 nm), the error can be pronounced. As seen, the typical lateral size measured in the AFM topography image in Fig. 4a is about 15 nm. AFM measurement on the height of the Ag nanoparticles, on the other hand, is accurate. Assuming the nanoparticle is near-spherical, the mean diameter of the Ag nanoparticles obtained from the height measurements is 2.9 ± 0.3 nm (see Fig. A-20 in the supporting information in Annex A). This is consistent with both the mass spectrometry measurement as shown in Fig. 2 and previous STM results [14]. It is interesting to note that the SEM image shown in Fig. 4b exhibits some degree of coalescence indicated by the Turing patterns. It has been reported in the literatures that a pristine Ag nanoparticle is prone to coalescence caused by the irradiation of the electron beam in SEM and TEM imaging process [16].

To demonstrate the SERS activity of this novel substrate, R6G was used as the reporter molecule. Substrate 3 was prepared under the same experimental condition as substrate 2 but on glass slide coated with Ag electrodes. The SERS spectrum of R6G was taken after immersing the substrate into a 70 nM aqueous solution of R6G for 30 seconds and drying in air shown in Fig. 5a. In comparison, no SERS spectrum observed on the vapour-deposited Ag electrode as shown in Fig. 5b.

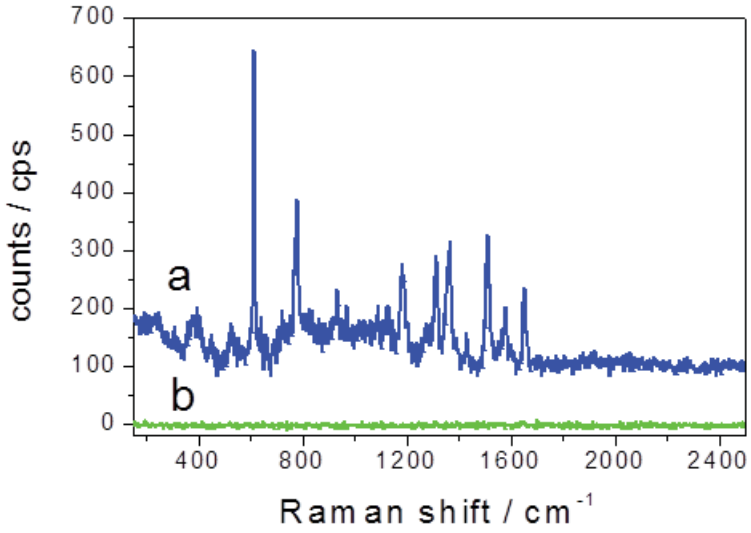

Figure 5 (a) SERS spectrum of R6G after immersing substrate 3 in 70 nM aqueous solution for 30 seconds (baseline corrected) with excitation laser 532 nm, 6 µW, 1 second acquisition time, (b) and a spectrum collected from the flat Ag electrode without nanoparticle shows no SERS activity. The spectra are offset for clarity.

Uniformity of the SERS Response of the Substrate

Uniform SERS response across the entire SERS substrate is desirable for quantifiable detection of chemical and biological molecules. It reflects on the reproducibility of SERS spectra recorded from different points of the same substrate. To demonstrate the uniformity of the SERS response across one substrate, a large-area substrate (substrate 4) with diameter of 1 cm was prepared on a glass slide under the same experimental condition as substrate 2. A randomly selected large area (200x155 µm) point-by-point Raman mapping was recorded with a step size of 1 µm and 0.2 second acquisition time per point. SERS spectra of R6G were taken after immersing substrate 4 into a 70 µM aqueous solution of R6G for 30 seconds and drying in air. A small section of 50x50 µm square (Fig. 6a, red box) within the imaged area was deliberately photobleached to show contrast. The sample was excited with 532 nm radiation. The 612 cm^{-1} vibrational band of R6G was used in constructing the hyperspectral image shown in Fig. 6b. The SERS signal is highly uniform across the large area outside the red box with a standard deviation of less than ±12%. Inside the red square, the SERS intensity is 42% lower which results in a higher standard deviation of ±16%. Other areas on the 1 cm-sized substrate all showed similar results (see Fig. A-21 in the supporting information in Annex A). These results demonstrate that performances of our SERS substrates are highly uniform and reproducible. Such uniformity is likely a result of an averaged SERS response from the highly distributed hot spots as a result of tightly packed silver nanoparticles under the 1 µm excitation spot. Moreover, uniformity in the interparticle distance of the between silver nanoparticles is the key factor in reproducible SERS response.

We also investigated the stability of our SERS substrate. Substrate 4 was prepared three weeks prior to the incubation of R6G solution. SERS response was monitored for seven weeks after the exposure (see Fig. A-21 in the supporting information in Annex A). No significant variation in SERS response was observed during the seven week period. The stability of the substrate is an important factor for practical application.

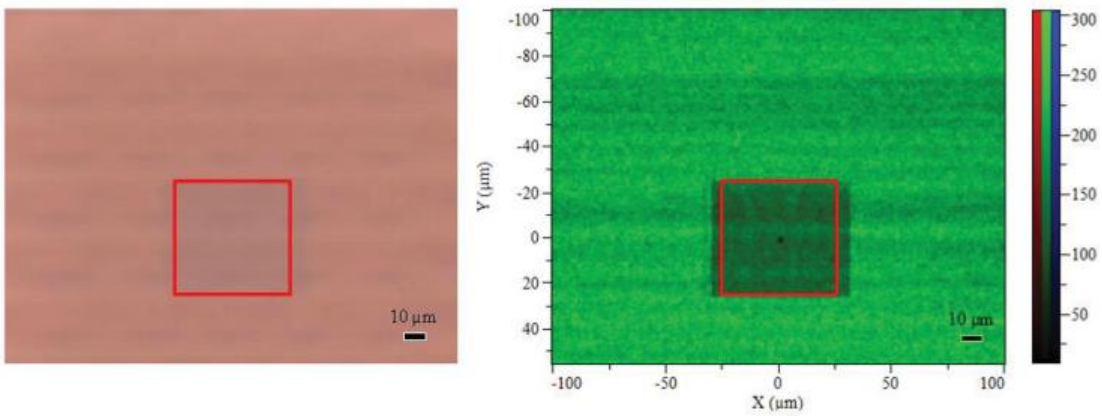

Figure 6 a) Optical image of the SERS substrate 4 after immersing in R6G 70 µM aqueous solution for 30 seconds and scanned in small area with excitation laser 532 nm, laser power 6 µW, each point 0.2 second. The substrate was prepared 3 weeks prior to the exposure to R6G. A small section - the red square (50x50 µm) was deliberately photo-bleached to show the contrast. It should be noted that the dark area is slightly larger than the red square in the horizontal direction resulted from the Raman instrument design to ensure correct data acquisition when the laser changes scan direction. The horizontal lines are artifacts in the optical image; and (b) SERS hyperspectral image reconstructed from the 612 cm^{-1} vibrational band of R6G. The image (b) is constructed from the same area of the SERS substrate as in (a). The scale bars in both images are 10 µm

Saturation Studies and Solvent Effect

To determine the optimal immersion time for the attachment of the Raman reporter molecule, we performed a series of saturation studies. Electrical and SERS measurements were performed on a SERS substrate after each subsequent exposure to 0.2 mM of 4-mercaptobenzonitrile (4-MBN) anhydrous ethanol solution for a set period of time. Substrate 5 was prepared on the electrode patterned glass slide. After each immersion, the substrate was removed from the solution, rinsed with anhydrous ethanol and dried under N_2 gas. The substrate was then measured for its electrical resistance across the silver electrode and SERS response from the Ag nanoparticle films. For each immersion time, 6 SERS spectra were acquired from different region of the Ag nanoparticle film. Each of the spectra below is an average of 6 spectra. This study was performed with the 633 nm excitation line.

The bottom spectrum in Fig 7 (left panel, black spectrum) was taken from the pristine substrate before incubation. This spectrum shows typical vibrational stretches of the carbonaceous species likely adsorbed on the film surface. The SERS signatures from pristine substrate are similar to the

graphitic carbon vibrational signatures and are typically consists of the graphitic and disordered bands at 1380 and 1607 cm^{-1}.

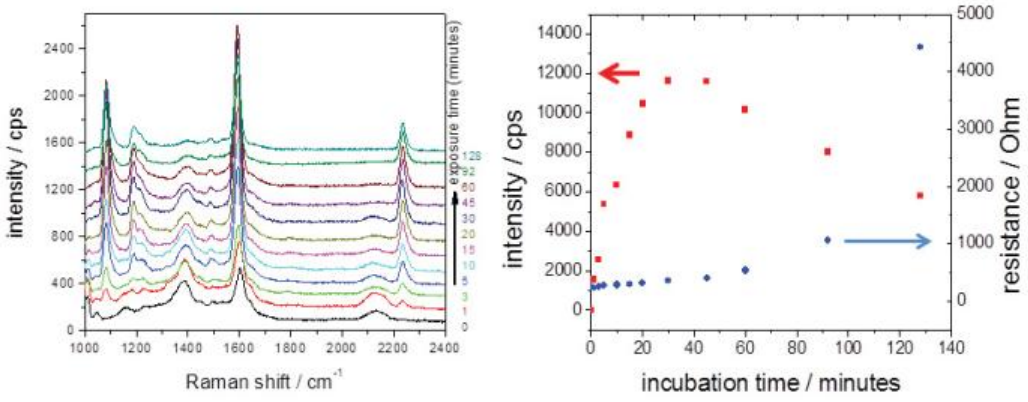

Figure 7 The left panel shows SERS spectra of substrate 5 immersed for various length of time in a 0.2 mM 4-MBN (Raman reporter molecule) solution. Right panel shows SERS response at 2200 cm^{-1} and resistance of the substrate at various incubation time. A significant increase in the resistance was observed after 60 minutes of incubation time.

In order to reduce the uncertainty in the SERS enhancement factor estimation, it is necessary that as much as possible of the carbonaceous adsorbates be cleaned off from the substrate before or during the attachment of the 4-MBN compound. As the pristine Ag nanoparticle film is prone to damage, cleaning steps such as UV-Ozone, chemical or plasma treatment on the film tends to incur damages to the film. Interestingly, the thiol functional group has strong affinity towards silver surfaces and has been shown to displace physisorbed species on silver during the formation of a self-assembled monolayer film.

Left panel of figure 7 shows the SERS response of substrate 5 from 1 to 128 minutes of immersion time. The 1585cm^{-1} ring mode of the Raman reporter molecule overlaps with the graphitic stretch of the carbonaceous SERS signature. However, the 2220 cm^{-1} stretch from the Raman reporter molecule does not overlap with any other carbonaceous Raman vibration and thus serves as a good indicator to assess the bonding of Raman reporter molecules.

Contrary, the decrease in signal intensity of the 1380 cm^{-1} (or 2130 cm^{-1} band can be used to gauge the amount of carbonaceous adsorbate being displaced or "cleaned-off" from the Ag nanostructures. Although the 2220 cm^{-1} band became visible almost immediately after immersion in the reporter solution (1-minute immersion, as shown in the red SERS spectrum in Fig. 7), the prominent presence of 1380 cm^{-1} band also indicated that most of the SERS features are dominated by the carbonaceous adsorbates. As incubation time increased so did the strength of the 2220 cm^{-1} band and this was accompanied by a decrease of the 1380 cm^{-1} band, indicative of the displacement of the carbonaceous adsorbates by the Raman reporter molecule, 4-MBN. After approximately 30 minutes of immersion time, the strength of the 2220 cm^{-1} levelled off up to 45 minutes. In fact, further increase in the immersion time seemed to show a very slight decrease in the SERS signature (for better visual effect, see the red square trace in the right panel of Fig. 7). It is possible that the silver film began to degrade past this immersion time period. This is corroborated by the accompanying electrical characterization of the nanosensor as shown by the

blue trace in the right panel of Fig. 7 and the change in the film morphology shown in SEM images (Fig. 8). As incubation time increases so does the resistance of the nanosensor, but one observes a dramatic jump beyond the 60 minutes incubation time which again indicates a change in the percolation networks that make up the conduction path across the silver nanoparticle films. Observable morphological changes can be seen in the SEM images. Although the SERS spectrum indicates that a certain amount of carbonaceous material was still present on the film surface at 45 minutes of immersion time, the spectra also showed that the amount of this material is far less as compared to the pristine substrates. Longer incubation times can remove even more physisorbed species from the substrate, but this would also causes damage to the film and render them less SERS active as indicated by the reduction in their SERS spectra, electrical response and change in film morphology. The 45 minutes of immersion time is thus used as the optimal time for obtaining the best SERS signature.

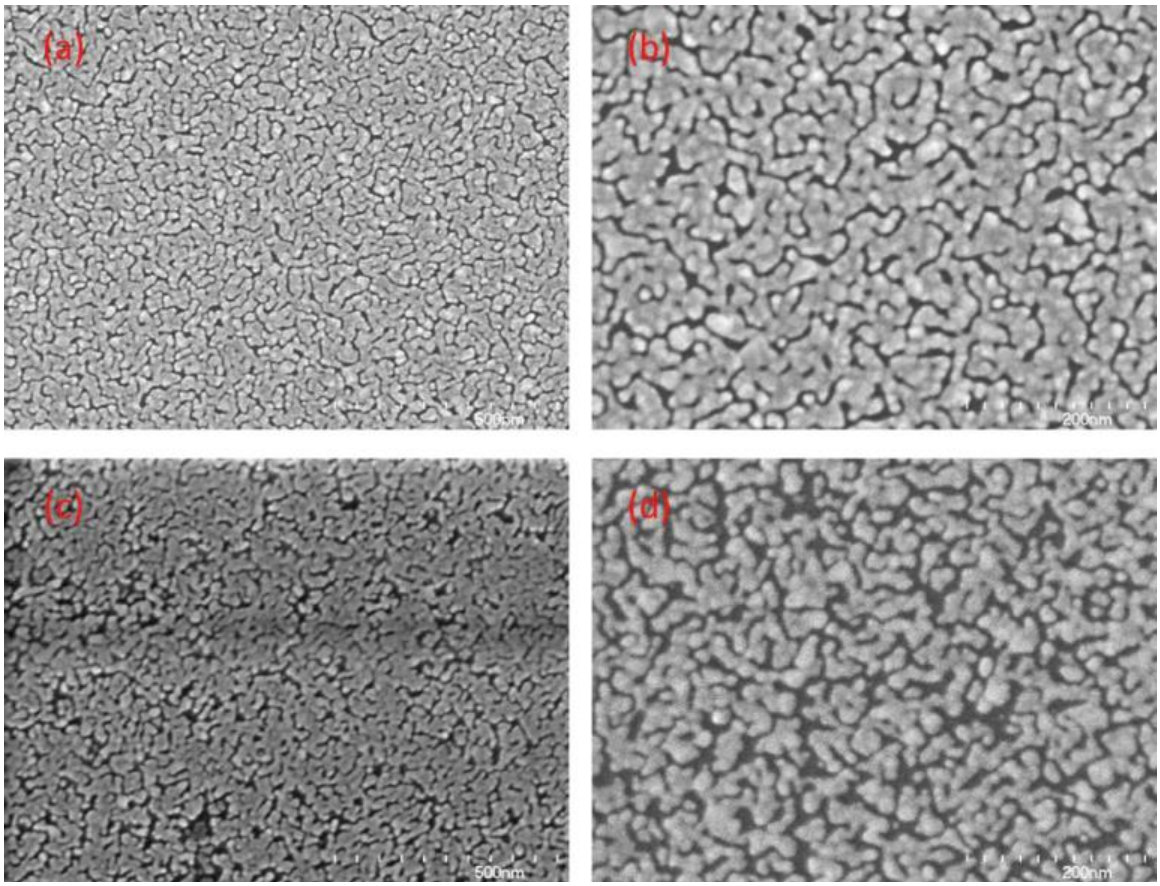

Figure 8 SEM images of the substrate 5 before (a and b) and after (c and d) 128 minutes of immersion in 0.2 mM of 4-MBN solution. Obvious changes to the film morphology were observed after 128 minutes of incubation time

Reproducibility of the SERS Response on Different Substrates

A set of three silver nanoparticle film substrates were prepared on electrode-patterned glass slides (substrates 6, 8, 10) and three similar films (substrates 7, 9 and 11) were prepared under the same experimental condition on the silicon wafer. All films were grown to full monolayer regime, similar to substrate 2 shown in Fig. 4. In their pristine state, substrates 6, 8 and 10 has a resistance of 21.2, 16.6 and 17.7 Ohm, respectively. After immersion in a 0.2 mM of 4-MBN solution for 45 minutes, the substrates resistance measured 21.9, 19.7 and 30.3 Ohm, respectively. All SERS reproducibility studies were performed with 130 μW of 632.8 nm excitation.

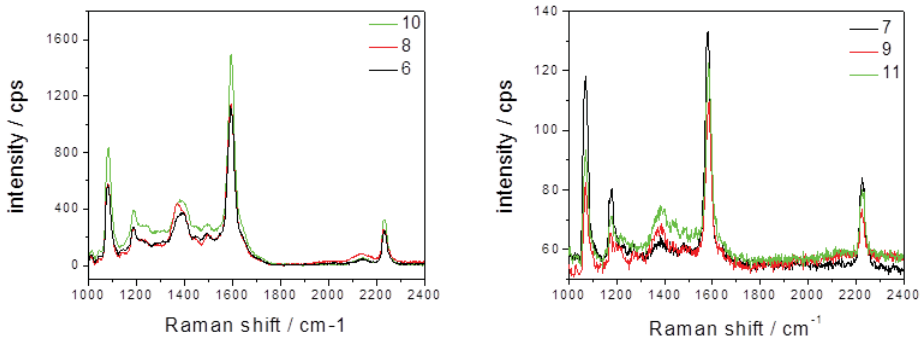

Figure 9 Reproducibility of six different SERS substrates. Left panel shows SERS response from substrates 6, 8 and 10 with Ag nanoparticles films deposited on glass slides. The right panel shows SERS response from substrates 7, 9 and 11 with similar Ag nanoparticle films deposited on the Si substrates. Each spectrum shown here is an average of 6 spectra taken from different locations on the nanosensor Ag film.

Figure 9 outlines SERS reproducibility from six different substrates prepared under similar deposition conditions. All six films exhibit similar electrical resistance. SERS responses from the glass substrates (substrates 6, 8 and 10) are shown in the left panel of Fig. 9 while the silver nanostructures fabricated on the silicon wafer are shown in the right panel. SERS spectra of substrates 6 and 8 reproduce very well (within a few percent). This is also reflected in their very similar electrical resistance post 4-MBN immersion, while substrate 10 which has a slightly higher electrical resistance also showed a slightly higher deviation in its SERS response. SERS spectrum obtained from substrate 10 is approximately 20% higher than the other two substrates. Substrates 7, 9, 11 were deposited on the p-dopped Si surface to facilitate SEM imaging. These substrates were also treated with 0.2 mM of 4-MBN solution for 45 minutes. Their SERS response varies by roughly 30% which is just slightly higher compared to those on glass. In general, the reproducibility is extremely good from both types of substrates. There is, however, a significant SERS intensity difference between the two sets of substrates. SERS responses from the substrates deposited on the Si are typically an order of magnitude lower than those on the glass. While difference in substrates can affect the overall response of the LSPR (and thus SERS) of the plasmonic film, the effect is expected to be small. The significant drop in the SERS response between these films may partly attributed to the morphological differences. Figure 10 below shows the SEM images of the substrates deposited on glass and Si substrates. Films deposited on the Si substrates appeared to be slightly more connected than those on the glass substrates. This may results in fewer SERS hot-sites (lost as the gaps joints to form connective network) thus lower SERS response. It is interesting to note that Tang et al. [17] fabricated

uniform Ag nanoparticle arrays on both ultrasmooth metallic and Si surfaces as SERS substrates. They found that the SERS signal on the metallic surface one order of magnitude higher than on the Si substrate. They attributed that to stronger plasmon coupling between the nanoparticles and their charge-conjugate images in the underlying metallic surface.

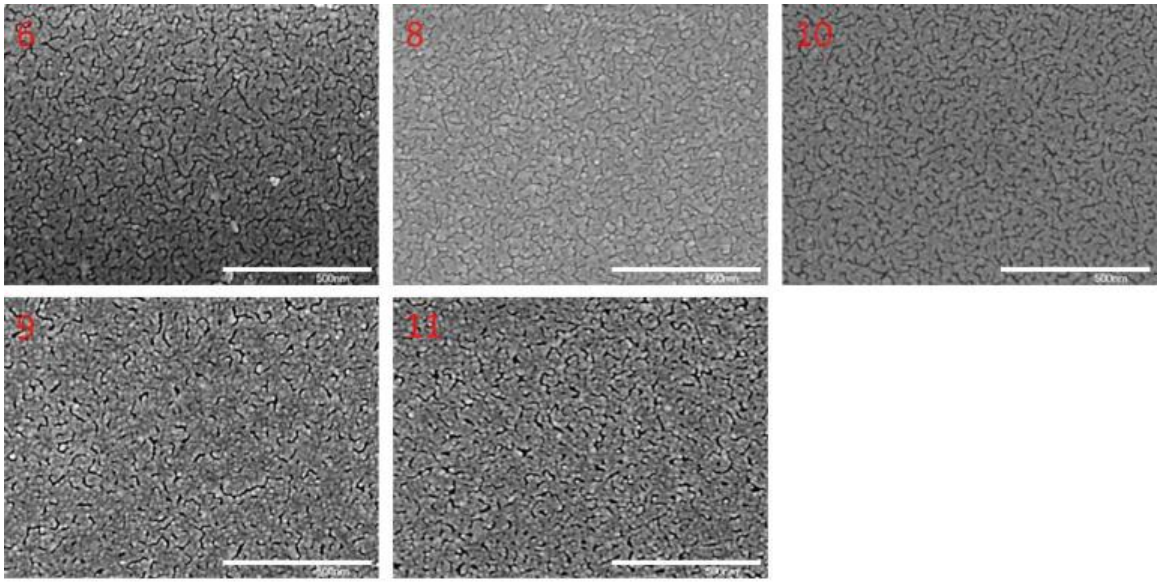

Figure 10 SEM images of substrates deposited on glass (6, 8, and 10) and on Si (9 and 11) before incubation.

Tunability of the SERS-active Substrates for Choice of Laser Excitation

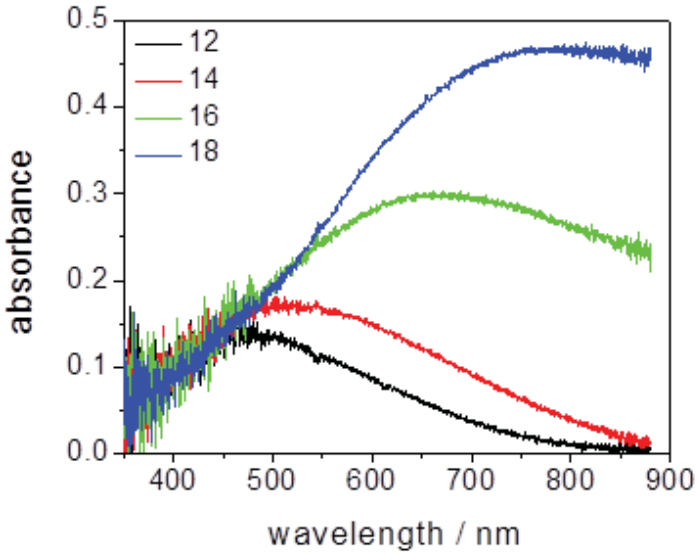

Figure 11 UV-VIS spectra of substrates 12, 14, 16, and 18.

Four substrates 12, 14, 16, and 18 of various nanoparticle densities were prepared with different deposition time ranging from low density to high density. We use these substrates to demonstrate the correlation between LSPR with SERS response as excited by 532 and 633 nm lasers. The UV-VIS spectra of these substrates are shown in Fig. 11. The LSPR peak positions of the substrates 12, 14, 16, and 18 are 488 nm, 520 nm, 650 nm and 770 nm, respectively. As indicated in our earlier studies, increasing interparticle coupling resulted in a red-shift of the LSPR. Our substrates can be continuously tuned in the visible range from 385 to 800 nm by controlling the interparticle distance through experimental control of deposition time. The LSPR of supported monodispersed silver nanoparticles is typically around 385 nm. This is in contrast to the silver island film on bare quartz (Ag/SiO_2) that the wavelength of LSPR peak (λ_{LSPR}) lies in the visible region of 444–506 nm with a very narrow adjustable range $\Delta\lambda_{LSPR} = 52$ nm [18].

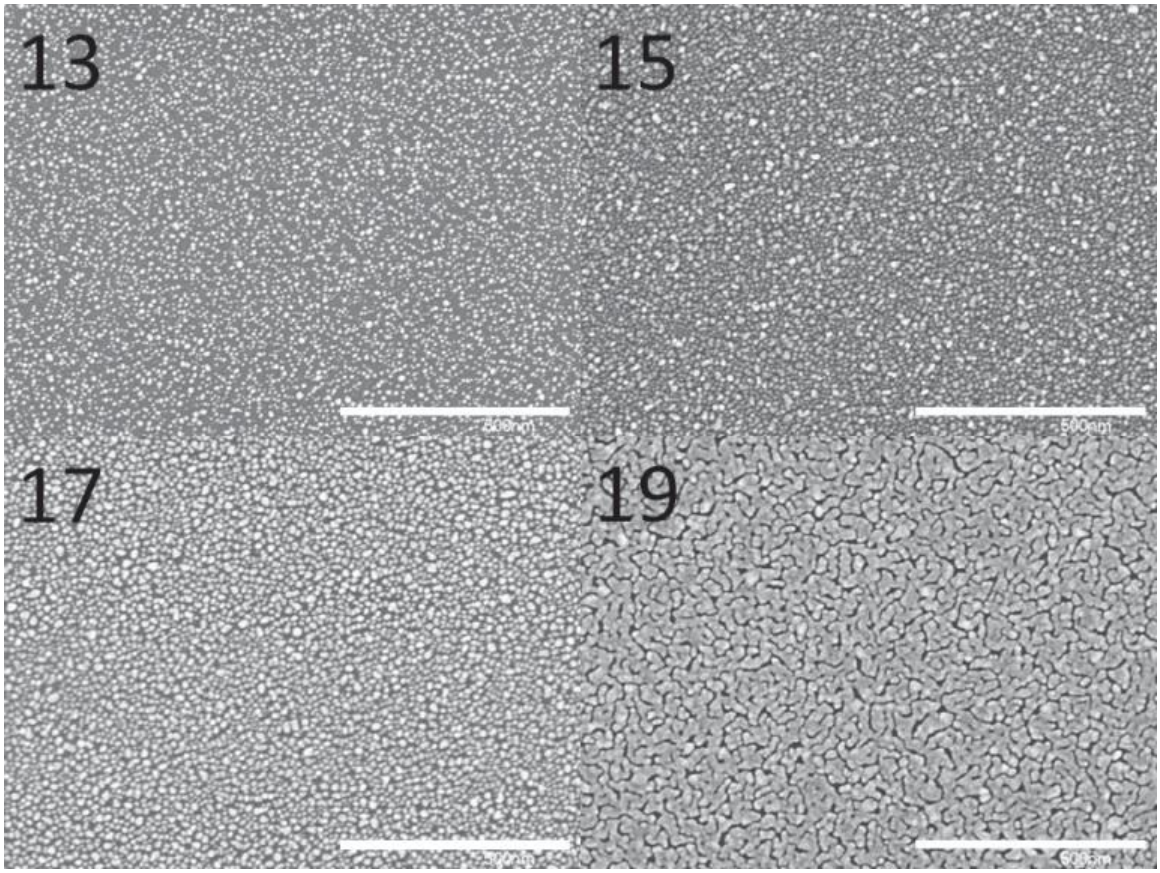

Figure 12 SEM images of Ag nanostructures on Si substrates 13, 15, 17 and 19 fabricated under same experimental conditions as substrates 12, 14, 16 and 18 on glass slides with deposition times of (a) 90, (b) 150, (c) 270 and (d) 450 seconds, respectively.

SEM imaging was conducted on substrates that were prepared under the same deposition time and experimental condition but on a p-dopped Si substrate to facilitate imaging. The SEM images of the four substrates in the pristine state are displayed in Fig. 12. As Fig. 12 shown, we have a good handle on controlling the nanoparticle density through deposition time. With increasing amount of Ag deposited on the substrates, the average distance between neighbouring particles decreased. It is interesting to note that, as the nanoparticle density on the surface increases, there

is an obvious change in topography of the nanostructured film. On substrate 12, the low particle density nanostructured film mainly composed of isolated individual nanoparticles. With increasing number of nanoparticles on the substrates 14 and 16, areas with aggregated or coalesced nanoparticles increased. On substrate 18, the nanoparticle film reached monolayer coverage on the glass and exhibited typical percolated Turing pattern similar to substrate 2 in Fig. 4b. Of note, the AFM image (Fig. 4a) of the percolated film revealed that the networked nanostructures are made of individual spherical nanoparticles with a height in good agreement of the nanoparticle size. It is possible that the coalescence of the Ag nanoparticles, at least partly, might have been caused by the energetic electron beam during the SEM imaging process [16]. There is one fundamental difference between these nanoparticle films and well known metal island films. The nanoparticles landed on the surface of the supports (glass or Si) self-assembled into a 2-dimentional film, one layer at a time [14]. The height of the nanoparticle film in a layer remained constant which was equal to the size of the nanoparticles (see Fig. A-20 in the supporting information in Annex A). The metal island films, on the other hand, grown in vertical and lateral dimensions [19][20].

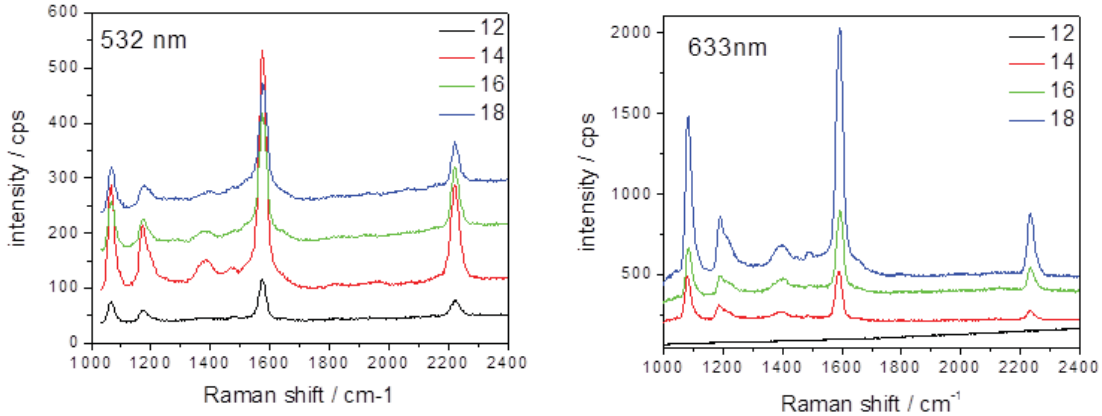

Figure 13 The left panel shows SERS spectra from substrates 12, 14, 16, 18 fabricated with 90, 150, 270 and 450 seconds deposition time. Samples were excited with a 532 nm laser at 30 µW where the right panel shows the response of the four substrates when excited with 632 nm light at 130 µW. Spectra are offset for clarity. The above spectra were obtained from a 1 µm diameter illumination circular spot.

Excitation and coupling of the LSPR in the coupled metal nanostructures are known to be the primary enhancement mechanism responsible for SERS. SERS enhancement maximizes when the wavelength of excitation source is close to the peak of the LSPR [21]. The SERS responses of the four substrates on glass were investigated after immersion in a 0.2 mM of 4-MBN solution for 45 minutes. SERS spectra were taken with both excitation sources 532 nm and 633 nm as shown in Fig. 13. While the SERS response is generally comparable in both 532 and 633 nm excitation, it is important to point out that the power density is 4 fold higher in the 633 nm excitation. Table 1 shows the intensity of the 2220 cm^{-1} band corrected to the same excitation density for all 4 substrates. It can be seen that substrate 14 showed the strongest SERS response with the 532 nm excitation while substrate 18 exhibited the strongest SERS signal with 633 nm. As the 532 nm excitation energy is closer to LSPR of the substrate 14 which was 520 nm as shown in the extinction spectra in Fig. 11 (trace a), it is not surprising that we observe a stronger SERS

response on it. Substrate 18, on the other hand, with a significantly red-shifted LSPR favoured the 633 nm excitation and thus resulted in a higher SERS intensity at this excitation. It is also interesting to point out that while we observed no SERS response with 633 nm excitation from substrate 12 which is largely composed of isolated Ag nanostructures, excitation with the 532 nm produces a weak but observable SERS response. This is in contrast to the Ag metal island film study by Van Duyne's Group which showed that the maximum SERS enhancement for different excitation sources at 488, 514, 641 and 722 nm all occurred at the same thickness (8 nm) of the films though the LSPR red-shifted with the increase of the thickness [19].

As the LSPR can be tuned continuously in the visible range from 385 nm to 800 nm, this approach provides ideal SERS substrates for different excitation lasers.

Table 1 SERS intensity of the 2220 cm^{-1} band corrected to the same excitation density for all 4 substrates with excitation of 532 nm and 633 nm, respectively.

Substrate ID	**I(2220 cm^{-1}) excited by 532 nm**	**I(2220 cm^{-1}) excited by 633 nm**
Substrate 12	$4.0x10^3$	NA
Substrate 14	$2.3x10^4$	$2.0x10^3$
Substrate 16	$1.7x10^4$	$4.8x10^3$
Substrate 18	$9.4x10^3$	$1.1x10^4$

SERS Enhancement Factor Estimation

Equation (1) outlined the parameters needed for the estimation of the *SERS EF*.

$$SERS\ EF = \frac{I(SERS) \times N(Raman)}{I(Raman) \times N(SERS)} \quad (1)$$

Where, *I(SERS)* and *I(Raman)* are the SERS intensities of the same vibrational band of a reporter molecule under the same excitation condition while *N(SERS)* and *N(Raman)* are the number of scatterers in the excitation volume.

To determine the SERS enhancement factor, it is necessary to characterize the particle number density on each SERS substrate. This is done by SEM as shown in Fig. 12. The SEM imaging was conducted on films deposited on the Si substrates. The Si SERS substrates were prepared under the same experimental conditions and as those deposited on the glass substrates in order to facilitate the particle density estimation. The particle density of the Ag-films on glass substrates was deduced from their equivalent Si substrates. For substrate 12, the particle density of the nanoparticle film is $4.3x10^3/\mu m^2$ and the total number of nanoparticles in the laser spot (1 μm in diameter) is therefore $3.4x10^3$. It is hard to measure the real nanoparticle number for the rest three substrates but it can be estimated by multiplying with deposition time ratio as we have demonstrated that the nanoparticle density is proportional to the deposition time [22]. The validation of this estimation method is also supported by the linear increase of the surface coverage measured by the SEM images versus deposition time. We assume monolayer coverage of 4-MBN molecules on the Ag nanoparticles allowing *N(SERS)* for all four substrates on glass

can be estimated. Considering the size of 4-MBN molecule of about 7 nm in diameter, each Ag nanoparticle can accommodate only one 4-MBN molecule. From our earlier work, we have also established the *I(Raman)/N(Raman)* ratio for the 4-MBN molecule under the 633 nm excitation. These numbers are summarized in Table 1. Following equation 1, the enhancement factor of the four substrates was estimated and listed in Table 2. No SERS signal were observable from substrate 12 thus no SERS EF estimation is assigned to substrate 12. This is not unexpected as the excitation wavelength of 633 nm is farther away from the LSPR response of substrate 12 which is primarily composed of uncoupled isolated nanoparticles. On the other hand, SERS response on substrate 12 as excited with 532 nm is significantly benefited from field enhancement of the red-shifted LSPR (Table 1).

It is also not surprising that the SERS EF of substrates 14, 16 and 18 are not very different, even though substrate 18 showed a much denser Ag nanoparticle film. In fact, the estimated gap between Ag nanoparticles even for the densest substrate 18 is still above 5 nm assuming uniform nanoparticle distribution on the surface. This gap is significantly large according to Xu et al. [23] and Le Ru et al. [24]. In this gap range, it is expected that the EF is between 10^5-10^7.

Table 2 Enhancement factor of the substrates 12, 14, 16 and 18 as excited by 633 nm and corrected for full power (13 mW excitation)

Substrate ID	I(SERS)	N(SERS)	I(Raman)/N(Raman)	SERS EF
Substrate 12	NA	$3.4x10^3$	$4.7x10^{-6}$	NA
Substrate 14	$2.1x10^5$	$5.7x10^3$	$4.7x10^{-6}$	$7.6x10^6$
Substrate 16	$4.5x10^5$	$1.0x10^4$	$4.7x10^{-6}$	$9.4x10^6$
Substrate 18	$1.1x10^6$	$1.7x10^4$	$4.7x10^{-6}$	$1.4x10^7$

Vapour Exposure Studies

In this section, the vapour exposure performance of the SERS substrate will be investigated. As outlined in earlier sections of this report, long time immersion of the Ag nanoparticle substrate in 0.2 mM of 4-MBN can causes a change in the film morphology. This effect is reflected by the change in both the electrical resistance across the nanoparticle film as well as the SEM images of the film after 2+ hours of immersion. Similar studies by monitoring both the SERS and electrical resistances of the SERS substrate have been carried out while exposing them to the vapour from 0.2 mM of 4-MBN solution. Substrates 20 and 21 were deposited on glass while substrate 22 were deposited on glass with coated electrodes under the same experimental condition

Figure 14 (black trace) shows the SERS response of substrate 20 before and after 20 hours of exposure to vapour from 0.2 mM of 4-MBN solution at the ambient (22 °C) condition. Again, the SERS spectrum prior to vapour exposure shows the typical vibrational modes from carbonaceous adsorbates. As the vapour pressure of 4-MBN under the ambient condition is very low ($9.7x10^{-3}$ Torr at 25 °C), the attachment of 4-MBN molecules and displacement of the carbonaceous adsorbates through vapour exposure is expected to take place at a much longer time scale, the 2220 cm^{-1} stretch was not observed in the SERS spectrum in the first two hours of exposure time. Even after 20 hours of vapour exposure under the ambient condition, only a small (~$9.3x10^2$ cps) 2220 cm^{-1} band was observed (Fig. 14, red trace). This is approximately an order of magnitude

lower compared to similar substrates (substrate 5 in Fig. 7) directly immersed in the 4-MBN solution. Also, significant graphitic signatures indicated that the majority of the carbonaceous adsorbates remained on the film surface. In order to increase the vapour pressure of 4-MBN in the cell, the vapour exposure for substrate 21 was carried out at an elevated temperature (40 °C) for the same length of time. The green trace in Fig. 14 showed a significant difference in its SERS response. The 2220 cm^{-1} band shows a count rate of $1.1x10^4$ cps which is over an order of magnitude larger compare to substrate 20 exposure under ambient condition for the same length of time. It is interesting to note that this intensity is the same as the immersion exposure (substrate 18 in Fig. 7 and Table 1) under the optimal length of exposure time (45 minutes). It also suggested that monolayer of 4-MBN molecules were formed in both cases.

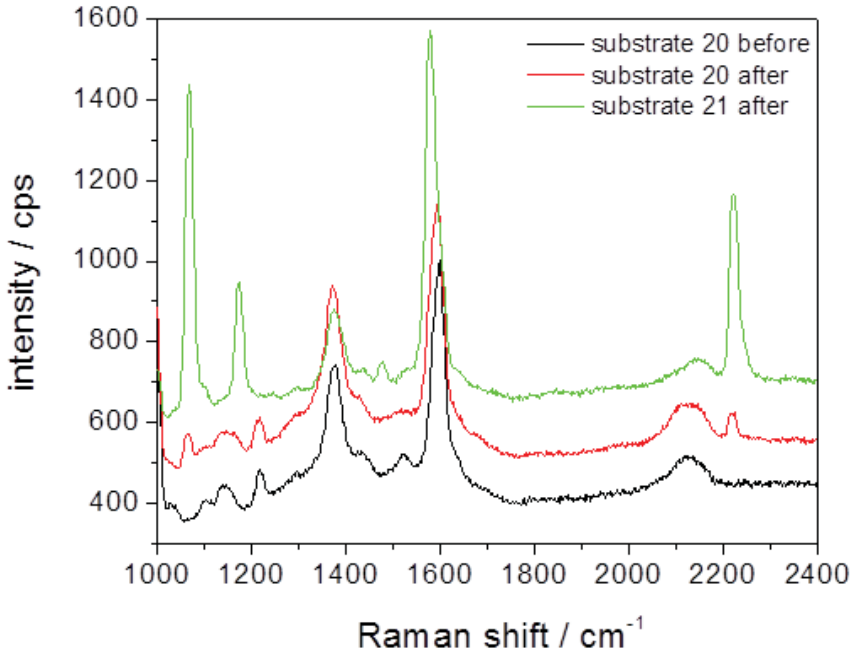

Figure 14 Vapour exposure studies of substrates 20 and 21. (a) The blue trace shows the SERS response of substrate 20 in its pristine state (as received); (b) The SERS response of substrate 20 after 20 hours of exposure to 0.2 mM of 4-MBN vapour under ambient condition; and (c) The SERS response of substrate 21 after 20 hours of exposure to 0.2 mM 4-MBN at elevated temperature (40 °C).

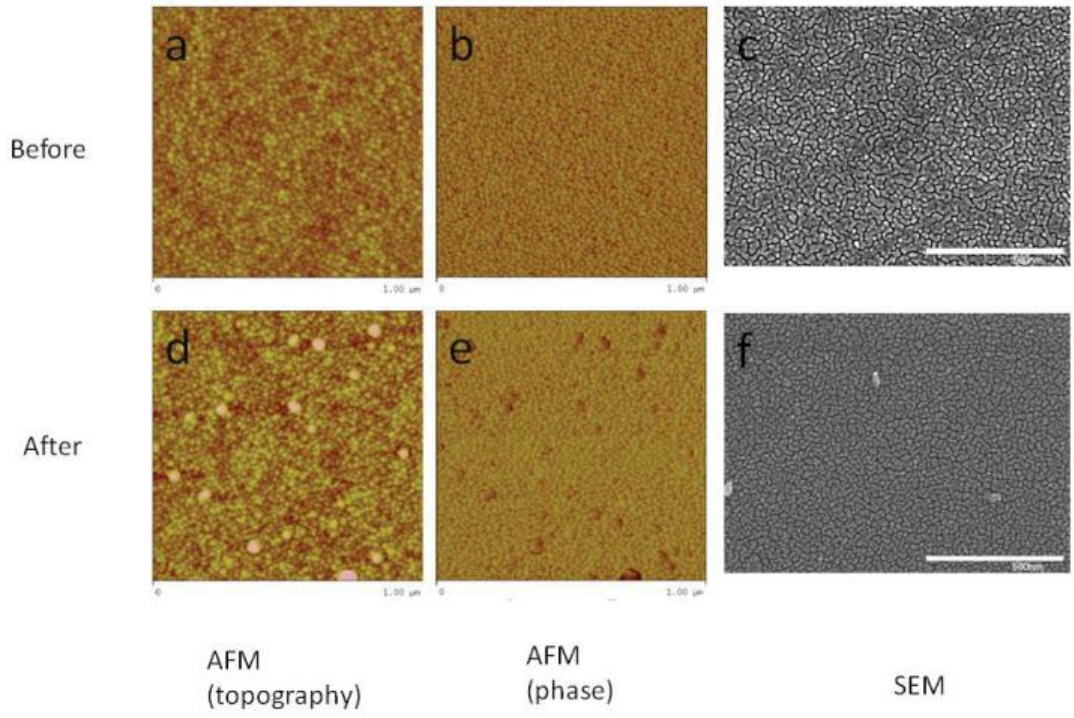

Figure 15 AFM topography (a and d) and phase (c and e) images and SEM images (c and f) of substrate 20 before (a, b and c) and after (d, e and f) 20 hours of exposure to 0.2 mM of 4-MBN vapour under ambient condition.

The vapour exposure effect on the Ag nanoparticle film morphology was examined by both AFM and SEM in Fig. 15. Images of substrates 20 and 21 were acquired before and after exposure to the 4-MBN vapour at 40 °C. Fig. 15 shows the AFM and SEM images of substrates 20 before and after the vapour exposure under ambient condition. It can be seen that even after 20 hours exposure, very little change was incurred on the nanostructured film and very small amount of 4-MBN molecules were absorbed on the surface. The mean roughness of the substrate only changed from 0.78 nm to 0.86 nm as revealed by the AFM topography images (Fig. 15 a and d). However, for the substrate 21 which was exposed to the 4-MBN vapour at elevated temperature, the mean roughness of the surface changed from 0.66 to 1.07 (Fig. 16 a and d). This suggested that the no significant damage was incurred on the nanostructured film even at elevated temperature. The AFM and SEM images also revealed that the nanoparticle surface was covered by a monolayer of 4-MBN molecules on substrate 21. This can be seen very clearly especially in the AFM phase images. It is known that the phase image has high contrast between the organic monolayer and the inorganic metal nanostructure. It is consistent with the fact that the SERS response (Fig. 14, green trace) after vapour exposure is equal to the maximum signal when incubated in the solution (Fig. 7).

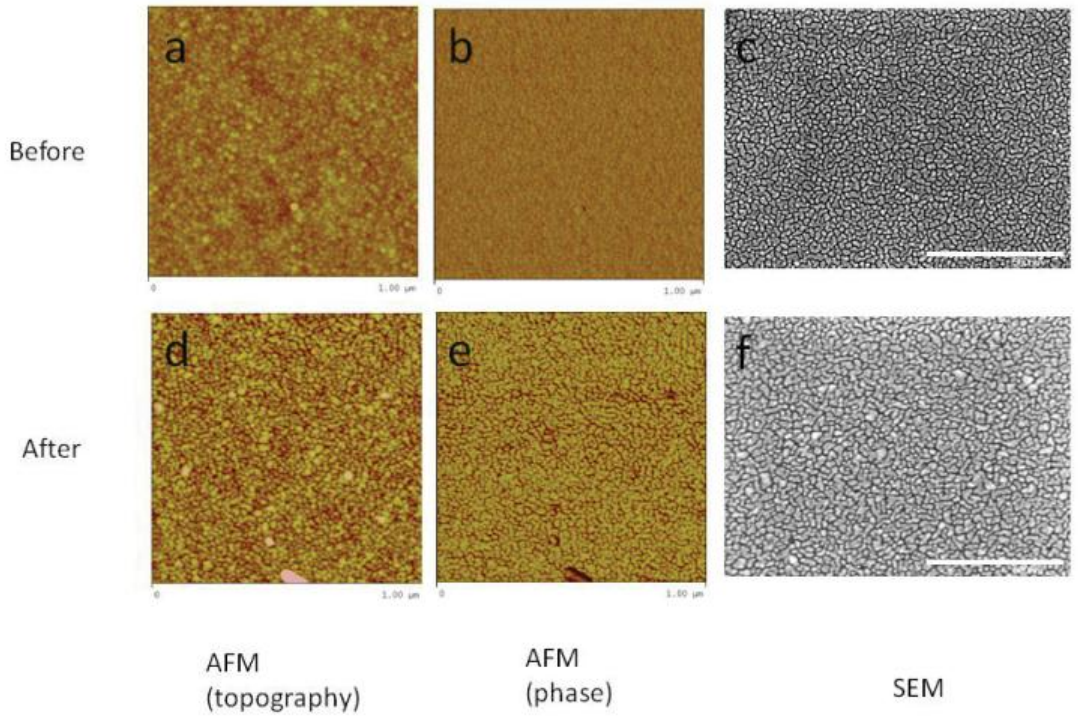

Figure 16 AFM topography (a and d) and phase (c and e) images and SEM images (c and f) of substrate 21 before (a, b and c) and after (d, e and f) 20 hours of exposure to 0.2 mM of 4-MBN vapour at elevated temperature (40 °C).

To find the optimal length of time for vapour exposure, substrate 22 was exposed to the vapour of 0.2 mM of 4-MBN at the elevated temperature by monitoring both the SERS and electrical resistances of the substrate while exposing them to the vapour from 0.2 mM of 4-MBN solution. The SERS spectra of substrate 22 exposed to 4-MBN vapour is shown in Fig. 17. It also shows the SERS intensity of 2200 cm^{-1} band and electrical resistances changes of substrate 22 exposed to the vapour of 0.2 mM of 4-MBN at the elevated temperature. While the SERS response steadily increases as the exposure time increases, electrical response of the substrate changed 200% in the first 60 minutes and then fluctuated up-and-down but remained within 24 to 36 kohm range. It is also interesting to point out that the SERS intensity reached to a maximum of $9.6x10^3$ cps at 400 minutes, similar to that with incubation exposure in solution for 45 minutes. Beyond this exposure length, SERS response dropped by 10% even though the electrical resistance does not show significant changes beyond this exposure time threshold. Similar to Fig. 15 and 16, the SEM images in Fig. 18 show a monolayer coverage of 4-MBN molecules on the substrate after 500 minutes of exposure to the 4-MBN vapour. The small drop of the SERS signal may be attributed to thicker coverage of 4-MBN molecules.

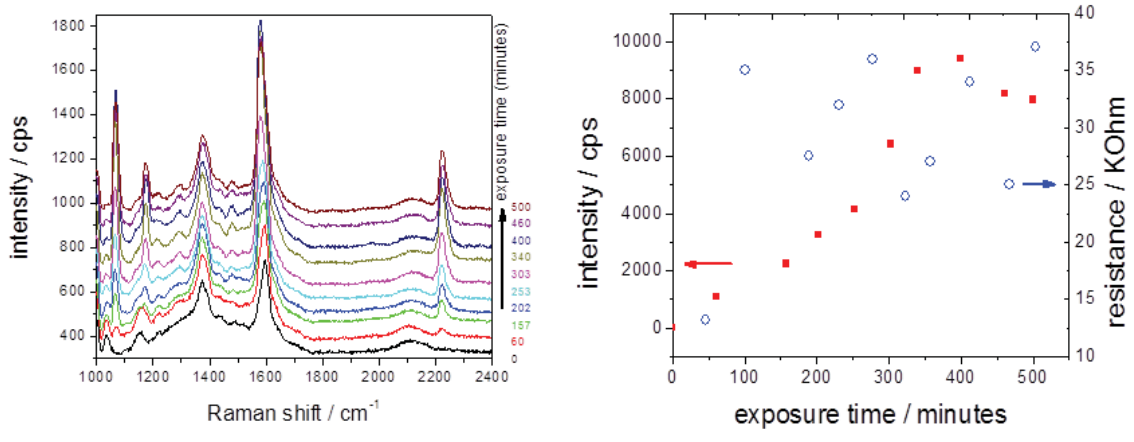

Figure 17 The left panel shows SERS spectra of substrate 22 exposed to 4-MBN vapour at an elevated temperature. SERS spectra (left panel) and electrical resistance response (right panel) of substrate 22 exposed to 4-MBN vapour at an elevated temperature (40°C).

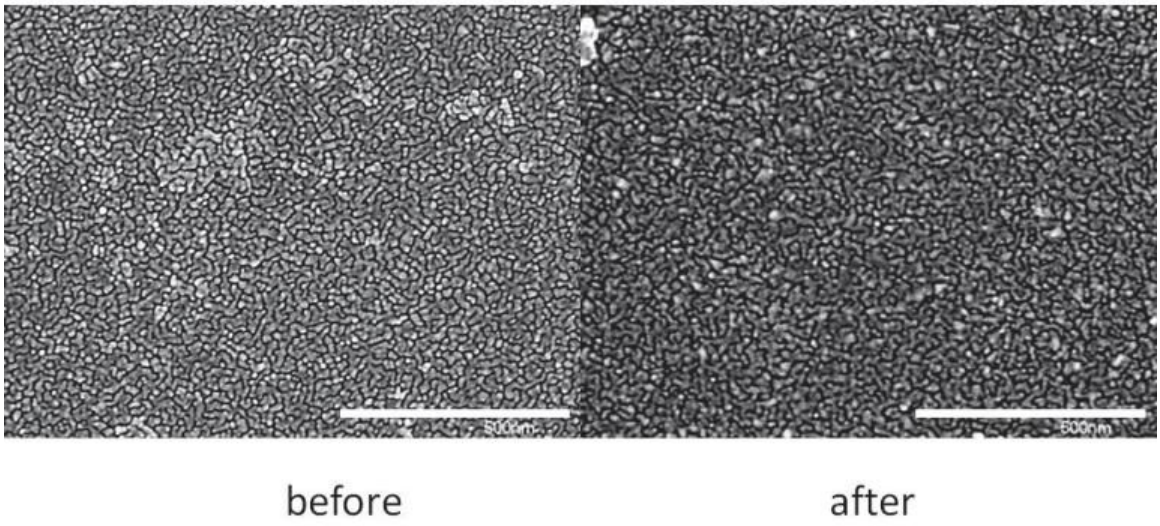

Figure 18 SEM images of substrate 22 before and after exposure to 4-MBN vapour at an elevated temperature (40°C) for 500 minutes.

This page intentionally left blank.

Conclusions

In summary, a SERS substrate was fabricated by self-assembly of gas phase generated negatively charged pristine Ag nanoparticle into a monodispersed 2-D film. This approach offers a highly uniform and reproducible substrate. Compared to the nano-lithographic approach, this approach is simple and cost effective. Unlike other SERS substrates, such as a vapour deposited metal island film, the LSPR of the Ag nanoparticle film can be continuously tuned from 385 to 800 nm in the visible range to match with the wavelength of the excitation laser for the benefit of optimized SERS enhancement. In addition, this approach provides a versatile SERS substrate for chemical and biochemical sensing in both liquid and vapour form, especially for molecule detection and identification in aqueous solution, as is essential for biological applications.

This page intentionally left blank.

References

[1] Fleischmann, M.; Hendra, P. J.; McQuillan, A. J. Journal of the Chemical Society-Chemical Communications 1973, 80–81.

[2] Jeanmaire, D. L.; Van Duyne, R. P. Journal Of Electroanalytical Chemistry And Interfacial Electrochemistry 1977, 84, 1–20.

[3] Albrecht M.G., Creighton J.A., Journal of the American Chemical Society 1977, 99, 5215

[4] Moskovits, M. The Journal of Chemical Physics 1978, 69, 4159.

[5] Sharma, B.; Frontiera, R. R.; Henry, A.; Ringe, E.; Duyne, R. P. V. Materials Today 2012, 15, 16–25.

[6] Fan, M.; Andrade, G. F. S.; Brolo, A. G. Analytica chimica acta 2011, 693, 7–25.

[7] Moskovits, M. Surface-Enhanced Raman Scattering – Physics and Applications, Topics Appl. Phys. 2006, 103, 1–18.

[8] Gersten J. I., Nitzan A. J. Chem. Phys. 1980, 73, 3023

[9] McCall S. L., Platzman P. M. Phys. Rev. B 1980, 22, 1660

[10] Etchegoin, P. G.; Ru, E. C. L. Surface Enhanced Raman Spectroscopy: Analytical, Biophysical and Life Science Applications; 2011, (Ed. Sebastian Schlücker) WILEY-VCH Verlag GmbH & Co. KGaA, Weinheim . pp.1-37.

[11] Otto A., Light Scattering in Solids IV, Topics in Applied Physics, 1984, 103 (eds M. Cardona. and G. Guntherodt.), Springer, Berlin, pp. 289–418.

[12] Nie S., Emory S. R. Science 1997, 275, 1102.

[13] Kneipp K., Wang Y., Kneipp H., Perelman L. T., Itzkan I., Dasari R. R., Feld M. S. Phys. Rev. Lett. 1997, 78, 1667.

[14] Pedersen, D. B.; Wang, S. The Journal of Physical Chemistry C 2009, 113, 4797–4803.

[15] Pedersen, D. B.; Wang, S. The Journal of Physical Chemistry C 2012, 116, 3258–3265

[16] Buffat, P. A. Philos. Trans. R. Soc. London, A 2003, 361, 291−295.

[17] Tang, J.; Ponizovskaya, E. V.; Bratkovsky, A. M.; Stewart, D. R.; Li, Z.; Williams, R. S. Nanotechnology 2008, 19, 415702.

[18] Xu, G.; Tazawa, M.; Jin, P.; Nakao, S. Applied Physics A 2004, 80, 1535–1540.

[19] Duyne, R. P. V.; Hulteen, J. C.; Treichelb, D. A. J. Chem. Phys. 1993, 99, 2101–2115.

[20] Oates, T. W. H.; Sugime, H.; Noda, S. The Journal of Physical Chemistry C 2009, 113, 4820–4828.

[21] Haynes, C. L.; Van Duyne, R. P. The Journal of Physical Chemistry B 2003, 107, 7426–7433.

[22] Pedersen, D. B.; Wang, S. J. Phys. Chem. C 2007, 111, 17493–17499.

[23] Xu, H.; Aizpurua, J.; Kall, M.; Apell, P. Physical review. E, 2000, 62, 4318–24.

[24] Le Ru, E. C.; Galloway, C.; Etchegoin, P. G. Physical chemistry chemical physics : PCCP 2006, 8, 3083–7.

Annex A Supporting information

A.1 SERS Spectra of DNA Bases on DRDC Substrates

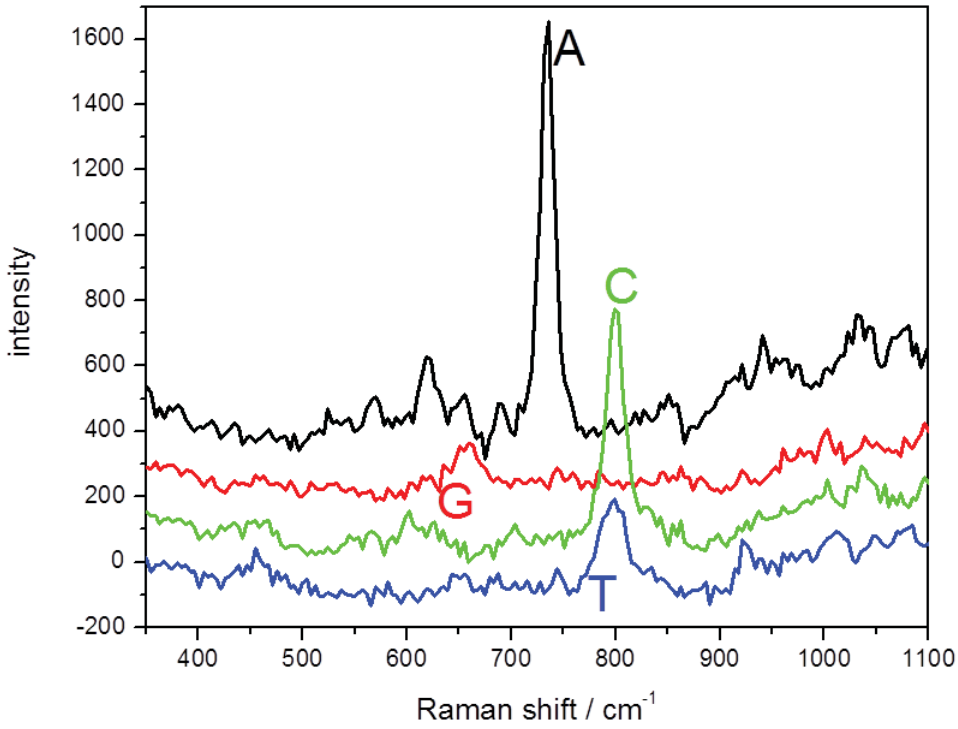

Figure A-19 SERS spectra of DNA bases A, G, C and T on DRDC SERS substrates after drying a 30 µL drop of 200 µM aqueous solution of each base. The SERS spectra were recorded at an excitation wavelength of 532 nm and a power of 108 µW.

A.2 Ag Nanoparticle Height Measured with AFM

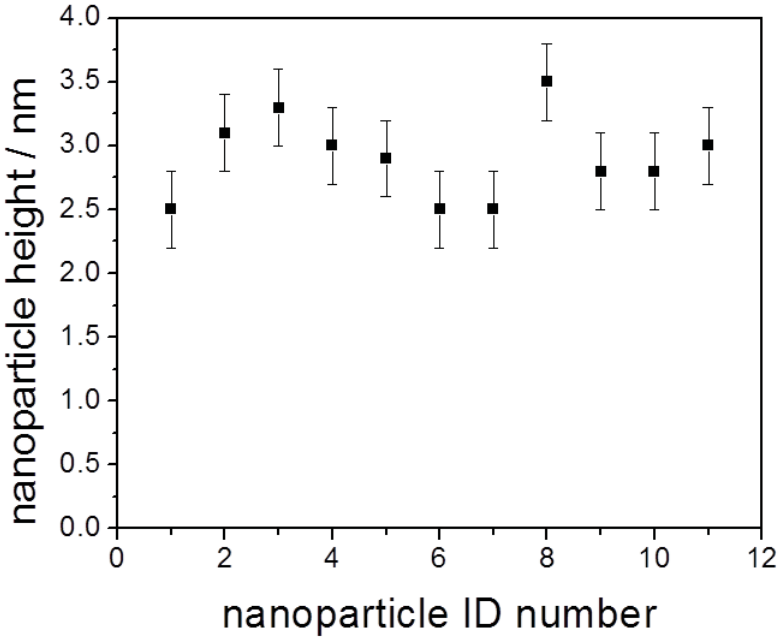

Figure A-20 Ag nanoparticle heights measured along a line in an AFM image.

A.3 Stability of SERS Substrates

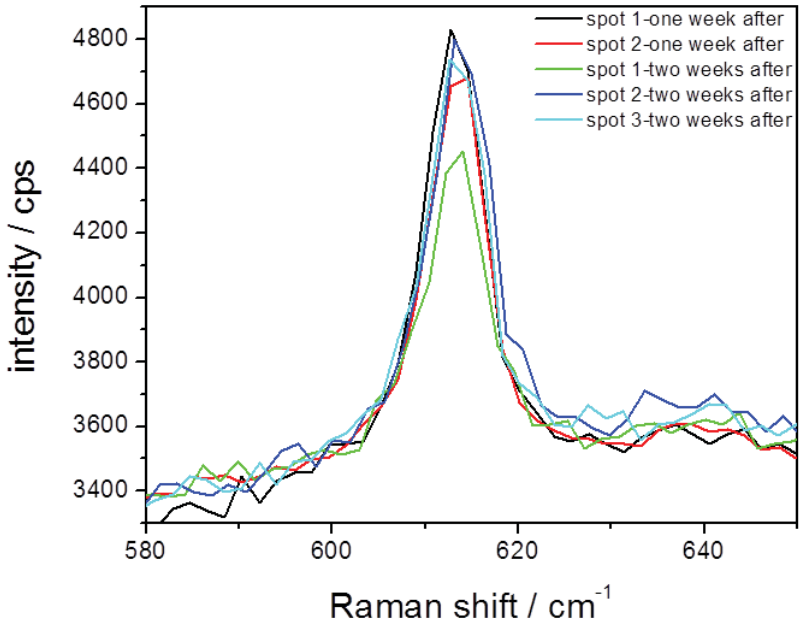

Figure A-21 SERS Spectra recorded one week and two weeks after the exposure of SERS substrate 4 to R6G 70 µM aqueous solution for 30 seconds. All spots were randomly selected on the 1 cm-sized substrate. The standard deviation is ±12% measured across the substrate two weeks after the exposure.

This page intentionally left blank.

DOCUMENT CONTROL DATA

(Security classification of title, body of abstract and indexing annotation must be entered when the overall document is classified)

1. ORIGINATOR (The name and address of the organization preparing the document. Organizations for whom the document was prepared, e.g. Centre sponsoring a contractor's report, or tasking agency, are entered in section 8.)

Defence R&D Canada – Suffield
P.O. Box 4000, Station Main
Medicine Hat, Alberta T1A 8K6

2. SECURITY CLASSIFICATION (Overall security classification of the document including special warning terms if applicable.)

UNCLASSIFIED
(NON-CONTROLLED GOODS)
DMC A
REVIEW: GCEC June 2010

3. TITLE (The complete document title as indicated on the title page. Its classification should be indicated by the appropriate abbreviation (S, C or U) in parentheses after the title.)

A Uniform, Reproducible and Tunable SERS Substrate for Chemical and Biological Sensing

4. AUTHORS (last name, followed by initials – ranks, titles, etc. not to be used)

Shiliang Wang; Lilin Tay; Henry Liu

5. DATE OF PUBLICATION (Month and year of publication of document.)	6a. NO. OF PAGES (Total containing information, including Annexes, Appendices, etc.)	6b. NO. OF REFS (Total cited in document.)
November 2013	46	24

7. DESCRIPTIVE NOTES (The category of the document, e.g. technical report, technical note or memorandum. If appropriate, enter the type of report, e.g. interim, progress, summary, annual or final. Give the inclusive dates when a specific reporting period is covered.)

Technical Memorandum

8. SPONSORING ACTIVITY (The name of the department project office or laboratory sponsoring the research and development – include address.)

Defence R&D Canada – Suffield
P.O. Box 4000, Station Main
Medicine Hat, Alberta T1A 8K6

9a. PROJECT OR GRANT NO. (If appropriate, the applicable research and development project or grant number under which the document was written. Please specify whether project or grant.)	9b. CONTRACT NO. (If appropriate, the applicable number under which the document was written.)
10ds01	

10a. ORIGINATOR'S DOCUMENT NUMBER (The official document number by which the document is identified by the originating activity. This number must be unique to this document.)	10b. OTHER DOCUMENT NO(s). (Any other numbers which may be assigned this document either by the originator or by the sponsor.)
DRDC Suffield TM 2012-164	

11. DOCUMENT AVAILABILITY (Any limitations on further dissemination of the document, other than those imposed by security classification.)

unlimited

12. DOCUMENT ANNOUNCEMENT (Any limitation to the bibliographic announcement of this document. This will normally correspond to the Document Availability (11). However, where further distribution (beyond the audience specified in (11) is possible, a wider announcement audience may be selected.))

unlimited

13. ABSTRACT (A brief and factual summary of the document. It may also appear elsewhere in the body of the document itself. It is highly desirable that the abstract of classified documents be unclassified. Each paragraph of the abstract shall begin with an indication of the security classification of the information in the paragraph (unless the document itself is unclassified) represented as (S), (C), (R), or . It is not necessary to include here abstracts in both official languages unless the text is bilingual.)

This report provides a novel approach to self-assemble negatively charged individual pristine silver nanoparticles generated in the gas phase (with diameter less than 10 nm) on to a solid support (glass, plastic, rubber, silicon wafer, ITO, etc.) for the fabrication of a low-cost SERS-active substrate. The SERS substrate has been demonstrated to be tunable to accommodate different excitation lasers to achieve the maximum SERS response simply by controlling the deposition time. The SERS response has been shown to be highly reproducible / uniform from point-to-point across the entire substrate as well as from batch-to-batch which is desirable for quantifiable detection of chemical and biological molecules. In addition, the DRDC SERS substrate works well for chemical and biochemical sensing in both liquid and vapour forms. This new technology provides an affordable and reliable sensing and identification capability against new and emerging chemical and biological threats in support of the CF.

Le présent rapport fournit une nouvelle approche concernant les nanoparticules d'argent pures individuelles chargées négativement et auto assemblées produites au cours de la phase gazeuse (diamètre de moins de 10 nm) sur un support solide (verre, plastique, caoutchouc, plaquette de silicium, oxyde d'étain et d'indium, etc.) pour la fabrication d'un substrat SERS (spectrométrie Raman améliorée par la surface) peu coûteux. On a démontré que le substrat SERS est réglable afin de pouvoir s'adapter à différents lasers d'excitation pour obtenir la réponse SERS maximale simplement en contrôlant le temps de dépôt. On a démontré que la réponse SERS est hautement reproductible et uniforme d'un point à l'autre dans tout le substrat et d'un échantillon à l'autre, ce qui est souhaitable pour la détection quantifiable de molécules chimiques et de molécules biologiques. De plus, le substrat SERS de RDDC est efficace pour la détection chimique et la détection biochimique sous forme liquide et sous forme de vapeur. Cette nouvelle technologie peut fournir une capacité d'identification et de détection fiable et abordable des menaces biologiques et des menaces chimiques nouvelles ou émergentes comme les agents non traditionnels (ANT) pour appuyer les Forces canadiennes (FC).

14. KEYWORDS, DESCRIPTORS or IDENTIFIERS (Technically meaningful terms or short phrases that characterize a document and could be helpful in cataloguing the document. They should be selected so that no security classification is required. Identifiers, such as equipment model designation, trade name, military project code name, geographic location may also be included. If possible keywords should be selected from a published thesaurus, e.g. Thesaurus of Engineering and Scientific Terms (TEST) and that thesaurus identified. If it is not possible to select indexing terms which are Unclassified, the classification of each should be indicated as with the title.)

SERS; hand held raman; detection and identification; TICs; WMD

Defence R&D Canada

Canada's Leader in Defence
and National Security
Science and Technology

R & D pour la défense Canada

Chef de file au Canada en matière
de science et de technologie pour
la défense et la sécurité nationale

www.drdc-rddc.gc.ca